

# DYNAMICAL AND OBSERVATIONAL CONSTRAINTS ON ADDITIONAL PLANETS IN HIGHLY ECCENTRIC PLANETARY SYSTEMS<sup>1</sup>

ROBERT A. WITTENMYER, MICHAEL ENDL, WILLIAM D. COCHRAN  
 McDonald Observatory, University of Texas at Austin, Austin, TX 78712

HAROLD F. LEVISON

Department of Space Studies, Southwest Research Institute, Boulder, CO 80302

*Accepted for publication in AJ*

## ABSTRACT

Long time coverage and high radial velocity precision have allowed for the discovery of additional objects in known planetary systems. Many of the extrasolar planets detected have highly eccentric orbits, which raises the question of how likely those systems are to host additional planets. We investigate six systems which contain a very eccentric ( $e > 0.6$ ) planet: HD 3651, HD 37605, HD 45350, HD 80606, HD 89744, and 16 Cyg B. We present updated radial-velocity observations and orbital solutions, search for additional planets, and perform test particle simulations to find regions of dynamical stability. The dynamical simulations show that short-period planets could exist in the HD 45350 and 16 Cyg B systems, and we use the observational data to set tight detection limits, which rule out additional planets down to a few Neptune masses in the HD 3651, HD 45350, and 16 Cyg B systems.

*Subject headings:* extrasolar planets – planetary dynamics – stars: planetary systems

## 1. INTRODUCTION

One surprising result that has come out of the more than 200 extrasolar planet discoveries to date is the wide range of eccentricities observed. Unlike our own Solar system, many of the extrasolar planets which are not tidally locked to their host stars have moderate eccentricities ( $e > 0.2$ ), and 15 planets have high eccentricities ( $e > 0.6$ ). These observations have spawned several theories as to the origin of highly eccentric extrasolar planets. One such method, planet-planet scattering, occurs when multiple jovian planets form several astronomical units (AU) from the host star and then interact, leaving one in an eccentric orbit and often ejecting the other (Rasio & Ford 1996). This method has been proposed to explain the architecture of the  $\nu$  And planetary system (Ford et al. 2005), which contains a hot Jupiter as well as two jovian planets in moderately eccentric orbits. Lin & Ida (1997) suggested a merger scenario in which inner protoplanets perturb each other and merge to form a single massive, eccentric planet with  $e \gtrsim 0.3$  and  $a \sim 0.5 - 1$  AU.

Interactions with stellar companions are another possible way to boost a planet's eccentricity. Of the 15 stars hosting a planet with  $e > 0.6$ , six are also known to possess stellar-mass companions in wide binary orbits: HD 3651 (Mugrauer et al. 2006; Luhman et al. 2007), HD 20782 (Desidera & Barbieri 2007), HD 80606, HD 89744 (Wilson et al. 2001; Mugrauer et al. 2004), 16 Cyg B, and HD 222582 (Raghavan et al. 2006). If the inclination angle between the planetary orbit and a stellar companion is large, the Kozai mechanism (Kozai

1962) can induce large-amplitude oscillations in the eccentricity of the planet (e.g. Malmberg et al. 2006). These oscillations can be damped by general relativistic effects and by interaction with other planets, and hence are most effective in systems with a single planet in an orbit  $a \gtrsim 1$  AU from the host star (Takeda & Rasio 2005). The Kozai mechanism has been suggested to explain the high eccentricity of 16 Cyg Bb (Holman et al. 1997; Mazeh et al. 1997) and HD 80606b (Wu & Murray 2003). Hauser & Marcy (1999) found the inclination of 16 Cyg B orbiting the system barycenter to lie between 100 and 160 degrees, where 90 degrees is an edge-on orientation. However, it is the difference in inclination between the orbital planes of the planetary and stellar companion that is critical in determining the importance of the Kozai mechanism, and the inclination of the planet's orbit is generally not known for non-transiting systems.

Of the 192 known planetary systems, 23 (12%) are multi-planet systems. Recent discoveries of additional objects in systems known to host at least one planet (Udry et al. 2007; Wittenmyer et al. 2007; Rivera et al. 2005; Vogt et al. 2005; McArthur et al. 2004; Santos et al. 2004) suggest that multiple-planet systems are common. Of particular interest are systems which host a jovian planet and a low-mass "hot Neptune," e.g. 55 Cnc (=HD 75732), GJ 876,  $\mu$  Arae (=HD 160691), Gl 777A (=HD 190360). Motivated by the discoveries of hot Neptunes in known planetary systems, we have undertaken an intensive survey of selected single-planet systems to search for additional low-mass companions. Three of the planetary systems discussed in this paper (HD 3651, HD 80606, HD 89744) are part of this campaign. The excellent radial-velocity precision of the High Resolution Spectrograph on the Hobby-Eberly Telescope (HET), combined with queue-scheduling, allow us to time the observations in such a way as to minimize phase gaps in the orbit of the known planet, and

Electronic address: robw@astro.as.utexas.edu

<sup>1</sup> Based on observations obtained with the Hobby-Eberly Telescope, which is a joint project of the University of Texas at Austin, the Pennsylvania State University, Stanford University, Ludwig-Maximilians-Universität München, and Georg-August-Universität Göttingen.

also to act quickly on potential new planet candidates. The use of the HET in this manner is discussed further in Cochran et al. (2004) with regard to the discovery of HD 37605b.

In this work, we aim to combine observational limits on additional planets in known planetary systems with dynamical constraints obtained by N-body simulations. The observations address the question: What additional planets are (or are not) in these systems? The dynamical simulations can answer the question: Where are additional planets possible? Section 2 describes the observations and the test particle simulations for six highly eccentric planetary systems: HD 3651, HD 37605, HD 45350, HD 80606, HD 89744, and 16 Cyg B. We have chosen these systems based on two criteria: (1) Each hosts a planet with  $e > 0.6$ , and (2) Each has been observed by the planet search programs at McDonald Observatory. In §3, we present and discuss the results of the updated orbital fits, dynamical simulations, and detection limit computations.

## 2. OBSERVATIONS AND DATA ANALYSIS

### 2.1. Radial-Velocity Observations

Five of the six stars considered in this work have been observed with the McDonald Observatory 9.2 m Hobby-Eberly Telescope (HET) using its High Resolution Spectrograph (HRS) (Tull 1998). A full description of the HET planet search program is given in Cochran et al. (2004). For 16 Cyg B, observations from McDonald Observatory were obtained only with the 2.7 m Harlan J. Smith (HJS) telescope; the long-term planet search program on this telescope is described in Wittenmyer et al. (2006). All available published data on these systems were combined with our data from McDonald Observatory in the orbit fitting procedures.

### 2.2. Numerical Methods

To place constraints on the architecture of planetary systems, we would like to know where additional objects can remain in stable orbits in the presence of the known planet(s). We performed test particle simulations using SWIFT<sup>2</sup> (Levison & Duncan 1994) to investigate the dynamical possibility of additional low-mass planets in each of the six systems considered here. Low-mass planets can be treated as test particles since the exchange of angular momentum with jovian planets is small. We chose the regularized mixed-variable symplectic integrator (RMVS3) version of SWIFT for its ability to handle close approaches between massless, non-interacting test particles and planets. Particles are removed if they are (1) closer than 1 Hill radius to the planet, (2) closer than 0.05 AU to the star, or (3) farther than 10 AU from the star. Since the purpose of these simulations is to determine the regions in which additional planets could remain in stable orbits, we set this outer boundary because the current repository of radial-velocity data cannot detect objects at such distances.

The test particle simulations were set up following the methods used in Barnes & Raymond (2004), with the exception that only initially circular orbits are considered in this work. For each planetary system, test par-

ticles were placed in initially circular orbits spaced every 0.002 AU in the region between 0.05-2.0 AU. We have chosen to focus on this region because the duration of our high-precision HET data is currently only 2-4 years for the objects in this study. The test particles were coplanar with the existing planet, which had the effect of confining the simulation to two dimensions. Input physical parameters for the known planet in each system were obtained from our Keplerian orbit fits described in § 3.1, and from recent literature for 16 Cyg B (Wittenmyer et al. 2007) and HD 45350 (Endl et al. 2006). The planetary masses were taken to be their minimum values ( $\sin i = 1$ ). The systems were integrated for  $10^7$  yr, following Barnes & Raymond (2004) and allowing completion of the computations in a reasonable time. We observed that nearly all of the test-particle removals occurred within the first  $10^6$  yr; after this time, the simulations had essentially stabilized to their final configurations.

## 3. RESULTS AND DISCUSSION

### 3.1. Updated Keplerian Solutions for 4 Systems

We present updated Keplerian orbital solutions for HD 3651b, HD 37605b, HD 80606b, and HD 89744b in Table 1. A summary of the data used in our analysis is given in Table 2, and the HET radial velocities are given in Tables 3-6. The velocity uncertainties given for the HET data represent internal errors only, and do not include any external sources of error such as stellar “jitter.” The parameters for the remaining two planets, HD 45350b and 16 Cyg Bb, are taken from Endl et al. (2006) and Wittenmyer et al. (2007), respectively. Radial velocity measurements from the HET are given for HD 45350 in Endl et al. (2006), and velocities for 16 Cyg B from the HJS telescope are given in Wittenmyer et al. (2007). As in Wittenmyer et al. (2007), all available published data were combined with those from McDonald, and the known planet in each system was fit with a Keplerian orbit using GaussFit (Jefferys et al. 1987), allowing the velocity offset between each data set to be a free parameter. Examination of the residuals to our Keplerian orbit fits revealed no evidence for additional objects in any of the six systems in this study.

The Saturn-mass ( $M \sin i = 0.2M_{\text{Jup}}$ ) planet HD 3651b was discovered by Fischer et al. (2003) using observations from Lick and Keck. We fit these data, which were updated in Butler et al. (2006), in combination with observations from the HJS and HET at McDonald Observatory. The HET data, which consist of multiple exposures per visit, were binned using the inverse-variance weighted mean value of the velocities in each visit. The standard error of the mean was added in quadrature to the weighted rms about the mean velocity to generate the error bar of each binned point ( $N=29$ ). The rms about the combined fit for each dataset is: Lick & Keck—6.6 m s<sup>-1</sup>, HET—9.4 m s<sup>-1</sup>, HJS—12.2 m s<sup>-1</sup>. The fitted orbital parameters for HD 3651b are of comparable precision to those reported in Butler et al. (2006), and agree within  $2\sigma$ . The recent discovery of a T dwarf companion to HD 3651 (Mugrauer et al. 2006; Luhman et al. 2007) prompts an interesting exercise: Can the radial-velocity trend due to this object be detected in the residuals after removing the planet? We detect a slope of  $-0.27 \pm 0.05$

<sup>2</sup> SWIFT is publicly available at <http://www.boulder.swri.edu/~hal/swift.html>.

$\text{m s}^{-1} \text{ yr}^{-1}$ , indicating that we are indeed able to discern a trend which is possibly due to the binary companion. However, the reduced  $\chi^2$  of the orbital solution is not significantly improved by the inclusion of a linear trend ( $\Delta\chi^2=0.18$ ). The parameters given in Table 1 were obtained from the fit which did not include a trend.

We present 23 new HET observations for HD 37605 obtained since its announcement by Cochran et al. (2004). The data now span a total of 1065 days. The best fit is obtained by including an acceleration of  $-20.5 \pm 2.1 \text{ m s}^{-1} \text{ yr}^{-1}$ , indicating a distant orbiting body. Such a finding would lend support to the hypothesis that very eccentric single-planet systems originate by interactions within a wide binary system. The shortest period that this outer companion could have and still remain consistent with the observed acceleration and its uncertainty over the timespan of the observations is about 40 yr, assuming a circular orbit. This object would then have a minimum mass in the brown dwarf range.

The planet orbiting HD 80606, first announced by Naef et al. (2001), is the most eccentric extrasolar planet known, with  $e = 0.933 \pm 0.001$  (Table 1). We have fit the CORALIE data in combination with the Keck data given in Butler et al. (2006) and 23 observations from HET. The extreme velocity variations induced by this planet greatly increase the sensitivity of orbit fits to the weighting of individual measurements. Since the uncertainties of the HET velocities given in Tables 3-6 represent internal errors only, we experimented with adding  $1\text{--}7 \text{ m s}^{-1}$  of radial-velocity “jitter” in quadrature before fitting the data for HD 80606. For all of these jitter values, the fitted parameters remained the same within their uncertainties. Table 1 gives the parameters derived from a fit which added  $3.5 \text{ m s}^{-1}$  of jitter (Butler et al. 2006) to the HET data. The rms about the combined fit is: CORALIE– $18.7 \text{ m s}^{-1}$ , HET– $7.5 \text{ m s}^{-1}$ , Keck– $5.6 \text{ m s}^{-1}$ . Butler et al. (2006) noted that the eccentricity  $e$  and the argument of periastron  $\omega$  had to be held fixed in their fit to the Keck data alone. However, the large number of measurements included in this work allowed GaussFit to converge with all parameters free.

For HD 89744b, we combine data from the HET with 6 measurements from the HJS telescope and Lick data from Butler et al. (2006). The HET data were binned in the same manner as for HD 3651, resulting in  $N=33$  independent visits. The rms about the combined fit for each dataset is: Lick– $17.1 \text{ m s}^{-1}$ , HET– $10.7 \text{ m s}^{-1}$ , HJS– $9.5 \text{ m s}^{-1}$ . As with HD 3651b, our derived parameters agree with those of Butler et al. (2006) within  $2\sigma$ . The scatter about our fit remains large, most likely due to the star’s early spectral type (F7V), which hinders precision radial-velocity measurements due to the smaller number of spectral lines. For example, the F7V star HD 221287 was recently found to host a planet (Naef et al. 2007); despite the superb instrumental precision of the HARPS spectrograph, that orbital solution has a residual rms of  $8.5 \text{ m s}^{-1}$ .

### 3.2. Test Particle Simulations

The results of the dynamical simulations are shown in Figures 1-3. The survival time of the test particles is plotted against their initial semimajor axis. As shown in Figure 1, the short-period planets HD 3651 and HD 37605 sweep clean the region inside of about 0.5 AU. In both

of these systems, however, a small number of test particles remained in low-eccentricity orbits near the known planet’s apastron distance, near the 1:2 mean-motion resonance (MMR). In the HD 3651 system, particles remained stable beyond about 0.6 AU, which is not surprising given the low mass of the planet. For HD 37605, two distinct strips of stability are seen in Fig. 1, corresponding to the 1:2 and 1:3 MMRs. The eccentricity of the test particles in the region of the 1:2 MMR oscillated between 0.00 and 0.06. Particles in 1:3 MMR oscillated in eccentricity with a larger range, up to  $e \sim 0.4$ , which is expected due to secular forcing. As with HD 3651, the region beyond about 0.8 AU was essentially unaffected by the planet.

Figure 2 shows the results for the HD 45350 and HD 80606 systems. The long period (963.6 days) and relatively large mass ( $M \sin i = 1.8 M_{\text{Jup}}$ ) of HD 45350b restricted stable orbits to the innermost 0.2 AU. These test particles oscillated in eccentricity up to  $e \sim 0.25$ . The  $4M_{\text{Jup}}$  planet orbiting HD 80606 removed all test particles to a distance of about 1.5 AU, and only beyond 1.75 AU did test particles remain in stable orbits for the duration of the simulation ( $10^7 \text{ yr}$ ). A region of instability is evident at 1.9 AU due to the 8:1 MMR. Figure 3 shows that HD 89744b eliminated all test particles except for a narrow region near the 8:3 resonance. For the 16 Cyg B system, only particles inside of about 0.3 AU remained stable, leaving open the possibility of short-period planets. The surviving particles oscillated in eccentricity up to  $e \sim 0.45$ , but these simulations treat the star as a point mass, and hence tidal damping of the eccentricity is not included. Our results are consistent with those of Menou & Tabachnik (2003), who investigated dynamical stability in extrasolar planetary systems and found that no test particles survived in the habitable zones of the HD 80606, HD 89744, and 16 Cyg B systems.

### 3.3. Detection Limits

Three of these systems (HD 3651, HD 80606, HD 89744) were monitored intensely with the HET as part of a larger effort to search for low-mass, short period planets. No evidence was found for any such objects in these or any of the six systems in this work. We then asked what limits can be set on additional planets using the high-precision HET data we have obtained. The procedure for determining companion limits was identical to the method described in Wittenmyer et al. (2006), except that in this work, the best-fit Keplerian orbit for the known planet (see § 3.1) was removed before performing the limits computations. In this way, we determined the radial-velocity amplitude  $K$  for which 99% of planets would have been detected in the residuals. The eccentricity of the injected test signals was chosen to be the mean eccentricity of the surviving particles from the simulations described in § 3.2. Only the regions in which test particles survived were considered in these limits computations.

The results of these computations were highly varied, reflecting the differing observing strategies employed for these six objects. In particular, HD 3651, HD 80606, and HD 89744 were monitored intensely with the HET as part of a search for short-period objects, whereas HD 37605 and HD 45350 were only observed sporadically after the known planet orbits were defined and published

(Cochran et al. 2004; Endl et al. 2006), and 16 Cyg B has only been observed with the HJS telescope at a frequency of at most once per month. The companion limits are shown in Figures 4-6; planets with masses above the solid line can be ruled out by the data with 99% confidence. Not surprisingly, the tightest limits were obtained for HD 3651 (Figure 4), which had a total of 195 measurements, including 29 independent HET visits. For periods less than about 1 year, we can exclude planets with  $M \sin i \gtrsim 2$  Neptune masses. Similar results were obtained for 16 Cyg B ( $N=161$ ), where the limits approach a Neptune mass (Figure 6). Since the detection limits generally improve with the addition of more data and with higher-quality data, we can define a quantity to measure the goodness of the limits. A simple choice would be  $N/\bar{\sigma}$ , where  $N$  is the total number of observations, and  $\bar{\sigma}$  is the mean uncertainty of the radial-velocity measurements. The values of  $N$  and  $\bar{\sigma}$  are given in Table 2.

In the HD 45350 system, the results of the dynamical simulations complement those of the detection limit determinations. Very tight limits are obtained in close orbits ( $a \lesssim 0.2$  AU). In this region, test particles were stable (Fig. 2) and our observations can exclude planets with  $M \sin i$  between about 1 and 4 Neptune masses. Similar results were obtained for the 16 Cyg B system, in which test particles remained stable inward of  $a \sim 0.3$  AU. In that region, planets of 1-3 Neptune masses can be excluded by our limits determinations (Fig. 6). In most of the limits determinations, there are multiple “blind spots” evident where the periodogram method failed to significantly recover the injected signals. Typically this occurs at certain trial periods for which the phase coverage of the observational data is poor, and often at the 1-month and 1-year windows.

For none of HD 37605 (Fig. 4), HD 80606 (Fig. 5), or HD 89744 (Fig. 6) could additional companions be ruled out below about  $0.7 M_{\text{Jup}}$ , and for most orbital periods tested, the limits were substantially worse. One possible explanation for this result is that the sampling of the observations was poorly distributed in phase for many of the injected test signals, making significant recovery by the periodogram method difficult. This is evidenced by the “jagged” regions in the plots. Also, the intrinsic scatter for those three systems was too large to permit tight limits determination. This is certainly reasonable for the F7 star HD 89744. The three systems with the best limits (HD 3651, HD 45350, and 16 Cyg B) also had the lowest rms scatter about their orbital solutions (mean= $8.9 \pm 1.4 \text{ m s}^{-1}$ ; Table 1). In contrast, the mean rms for the remaining three systems was  $13.7 \pm 0.6 \text{ m s}^{-1}$ . Additional factors such as a paucity of data (HD 37605) and short time baselines (HD 80606, HD 89744) made the determination of useful companion limits challenging for some of the planetary systems in this study.

#### 4. SUMMARY

We have shown that for a sample of six highly eccentric extrasolar planetary systems, there is no evidence for additional planets. Test particle simulations show that there are regions detectable by current surveys (i.e. for  $a < 2$  AU) where additional objects can exist. For HD 3651 and HD 37605, we find that protected resonances are also present. Combining these simulations

with detection limits computed using new high-precision HET data combined with all available published data is particularly effective for the HD 3651 and HD 45350 systems. Additional short-period planets can be ruled out down to a few Neptune masses in the dynamically stable regions in these systems.

This material is based upon work supported by the National Aeronautics and Space Administration under Grant Nos. NNG04G141G and NNG05G107G issued through the Terrestrial Planet Finder Foundation Science program. We are grateful to the HET TAC for their generous allocation of telescope time for this project. We also would like to thank Barbara McArthur for her assistance with GaussFit software. We thank the referee, Greg Laughlin, for his careful review of this manuscript. This research has made use of NASA’s Astrophysics Data System (ADS), and the SIMBAD database, operated at CDS, Strasbourg, France. The Hobby-Eberly Telescope (HET) is a joint project of the University of Texas at Austin, the Pennsylvania State University, Stanford University, Ludwig-Maximilians-Universität München, and Georg-August-Universität Göttingen. The HET is named in honor of its principal benefactors, William P. Hobby and Robert E. Eberly.

## REFERENCES

- Barnes, R., & Raymond, S. N. 2004, *ApJ*, 617, 569
- Butler, R. P., et al. 2006, *ApJ*, 646, 505
- Cochran, W. D., et al. 2004, *ApJ*, 611, L133
- Desidera, S., & Barbieri, M. 2007, *A&A*, 462, 345
- Eggenberger, A., Udry, S., & Mayor, M. 2004, *A&A*, 417, 353
- Endl, M., Cochran, W. D., Wittenmyer, R. A., & Hatzes, A. P. 2006, *AJ*, 131, 3131
- Fischer, D. A., Butler, R. P., Marcy, G. W., Vogt, S. S., & Henry, G. W. 2003, *ApJ*, 590, 1081
- Ford, E. B., Lystad, V., & Rasio, F. A. 2005, *Nature*, 434, 873
- Goldreich, P., & Sari, R. 2003, *ApJ*, 585, 1024
- Hauser, H. M., & Marcy, G. W. 1999, *PASP*, 111, 321
- Holman, M., Touma, J., & Tremaine, S. 1997, *Nature*, 386, 254
- Jefferys, W. H., Fitzpatrick, M. J., & McArthur, B. E. 1987, *Celestial Mechanics*, 41, 39
- Kozai, Y. 1962, *AJ*, 67, 591
- Levison, H. F., & Duncan, M. J. 1994, *Icarus*, 108, 18
- Lin, D. N. C., & Ida, S. 1997, *ApJ*, 477, 781
- Lomb, N. R. 1976, *Ap&SS*, 39, 447
- Luhman, K. L., et al. 2007, *ApJ*, 654, 570
- Malmberg, D., Davies, M. B., & Chambers, J. E. 2007, *MNRAS*, L18
- Mazeh, T., Krymolowski, Y., & Rosenfeld, G. 1997, *ApJ*, 477, L103
- McArthur, B. E., et al. 2004, *ApJ*, 614, L81
- Menou, K., & Tabachnik, S. 2003, *ApJ*, 583, 473
- Mugrauer, M., Neuhäuser, R., Mazeh, T., Guenther, E., & Fernández, M. 2004, *Astronomische Nachrichten*, 325, 718
- Mugrauer, M., Seifahrt, A., Neuhäuser, R., & Mazeh, T. 2006, *MNRAS*, 373, L31
- Naef, D., et al. 2001, *A&A*, 375, L27
- Naef, D., et al. 2007, *A&A*, in press, arXiv:0704.0917
- Raghavan, D., Henry, T. J., Mason, B. D., Subasavage, J. P., Jao, W.-C., Beaulieu, T. D., & Hambly, N. C. 2006, *ApJ*, 646, 523
- Rasio, F. A., & Ford, E. B. 1996, *Science*, 274, 954
- Rivera, E., & Haghighipour, N. 2007, *MNRAS*, 374, 599
- Rivera, E. J., et al. 2005, *ApJ*, 634, 625
- Santos, N. C., et al. 2004, *A&A*, 426, L19
- Scargle, J. D. 1982, *ApJ*, 263, 835
- Takeda, G., & Rasio, F. A. 2005, *ApJ*, 627, 1001
- Tull, R. G. 1998, *Proc. SPIE*, 3355, 387
- Udry, S., et al. 2007, *A&A*, submitted, arXiv:0704.3841
- Vogt, S. S., Butler, R. P., Marcy, G. W., Fischer, D. A., Henry, G. W., Laughlin, G., Wright, J. T., & Johnson, J. A. 2005, *ApJ*, 632, 638
- Wilson, J. C., Kirkpatrick, J. D., Gizis, J. E., Skrutskie, M. F., Monet, D. G., & Houck, J. R. 2001, *AJ*, 122, 1989
- Wittenmyer, R. A., Endl, M., Cochran, W. D., Hatzes, A. P., Walker, G. A. H., Yang, S. L. S., & Paulson, D. B. 2006, *AJ*, 132, 177
- Wittenmyer, R. A., Endl, M., & Cochran, W. D. 2007, *ApJ*, 654, 625
- Wu, Y., & Murray, N. 2003, *ApJ*, 589, 605

TABLE 1  
KEPLERIAN ORBITAL SOLUTIONS

Planet	Period (days)	$T_0$ (JD-2400000)	$e$	$\omega$ (degrees)	K (m s <sup>-1</sup> )	M sin $i$ (M <sub>Jup</sub> )	$a$ (AU)	rms m s <sup>-1</sup>
HD 3651 b	62.197±0.012	53932.2±0.4	0.630±0.046	250.7±6.3	15.6±1.1	0.20±0.01	0.280±0.006	7.1
HD 37605 b	55.027±0.009	52992.8±0.1	0.677±0.009	218.4±1.7	201.5±3.9	2.39±0.12	0.263±0.006	13.0
HD 45350 b	963.6±3.4	51825.3±7.1	0.778±0.009	343.4±2.3	58.0±1.7	1.79±0.14	1.92±0.07	9.1
HD 80606 b	111.428±0.002	53421.928±0.004	0.933±0.001	300.4±0.3	470.2±2.5	4.10±0.12	0.460±0.007	13.5
HD 89744 b	256.78±0.05	53816.1±0.3	0.689±0.006	194.1±0.6	263.2±3.9	7.92±0.23	0.91±0.01	14.4
16 Cyg B b	799.5±0.6	50539.3±1.6	0.689±0.011	83.4±2.1	51.2±1.1	1.68±0.07	1.68±0.03	10.6

TABLE 2  
SUMMARY OF RADIAL-VELOCITY DATA

Star	$N$	$\bar{\sigma}$ (m s <sup>-1</sup> )	$\Delta T$ (days)	Source
HD 3651	163	3.4		Butler et al. (2006)
HD 3651	3	6.1		HJS <sup>a</sup>
HD 3651	29	2.1		HET <sup>b</sup>
HD 3651 (total)	195	3.2	7083	
HD 37605 (total)	43	2.9	1065	HET
HD 45350	38	2.8		Butler et al. (2006)
HD 45350	28	4.2		HET
HD 45350	47	8.9		HJS
HD 45350 (total)	113	5.7	2265	
HD 80606	61	13.7		Naef et al. (2001)
HD 80606	46	5.1		Butler et al. (2006)
HD 80606	23	2.5		HET
HD 80606 (total)	130	8.7	2893	
HD 89744	50	11.2		Butler et al. (2006)
HD 89744	33	3.2		HET
HD 89744	6	9.4		HJS
HD 89744 (total)	89	8.1	2687	
16 Cyg B	95	6.3		Butler et al. (2006)
16 Cyg B	29	19.7		HJS Phase II <sup>c</sup>
16 Cyg B	37	7.4		HJS Phase III
16 Cyg B (total)	161	9.0	6950	

<sup>a</sup> McDonald Observatory 2.7 m Harlan J. Smith Telescope. <sup>b</sup> McDonald Observatory 9.2 m Hobby-Eberly Telescope. <sup>c</sup> Phase II indicates an earlier instrument setup detailed in Wittenmyer et al. (2006). Phase III is the current configuration.

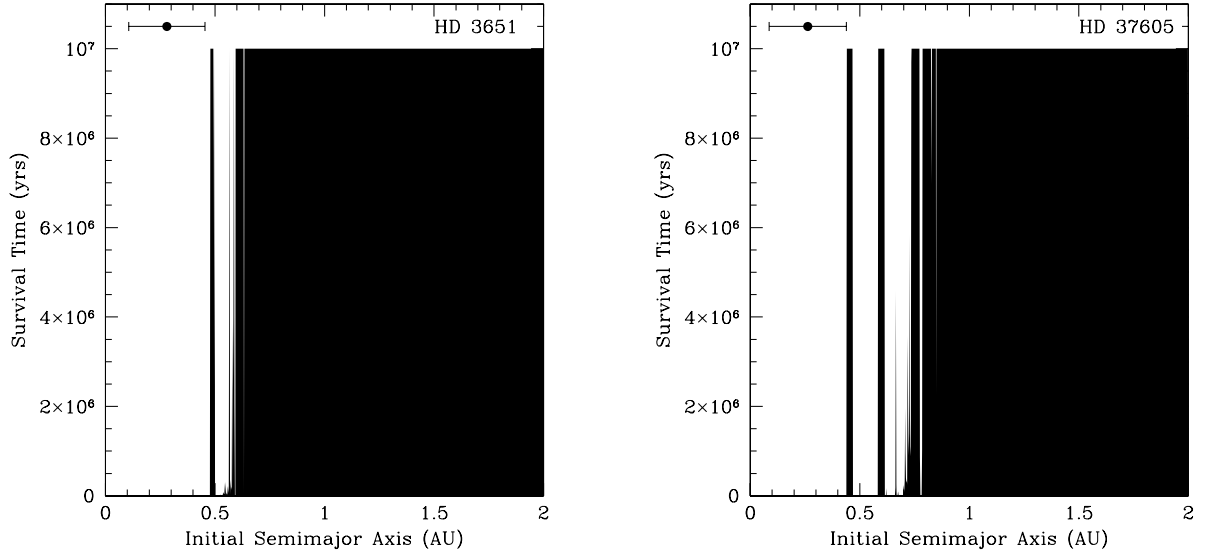


FIG. 1.— Left panel: Survival time as a function of initial semimajor axis for test particles in the HD 3651 system after  $10^7$  yr. The filled regions indicate test particles which survived. The orbital excursion of HD 3651b is indicated by the horizontal error bars at the top. Particles were placed on initially circular orbits with  $0.05 < a < 2.00$  AU. For all systems, the known planet removed particles which crossed its orbit. The dark region near 0.5 AU shows the stable 1:2 mean-motion resonance (MMR). Right panel: Same, but for the HD 37605 system. The dark regions near 0.45 AU and 0.6 AU show the stable 1:2 and 1:3 MMRs.

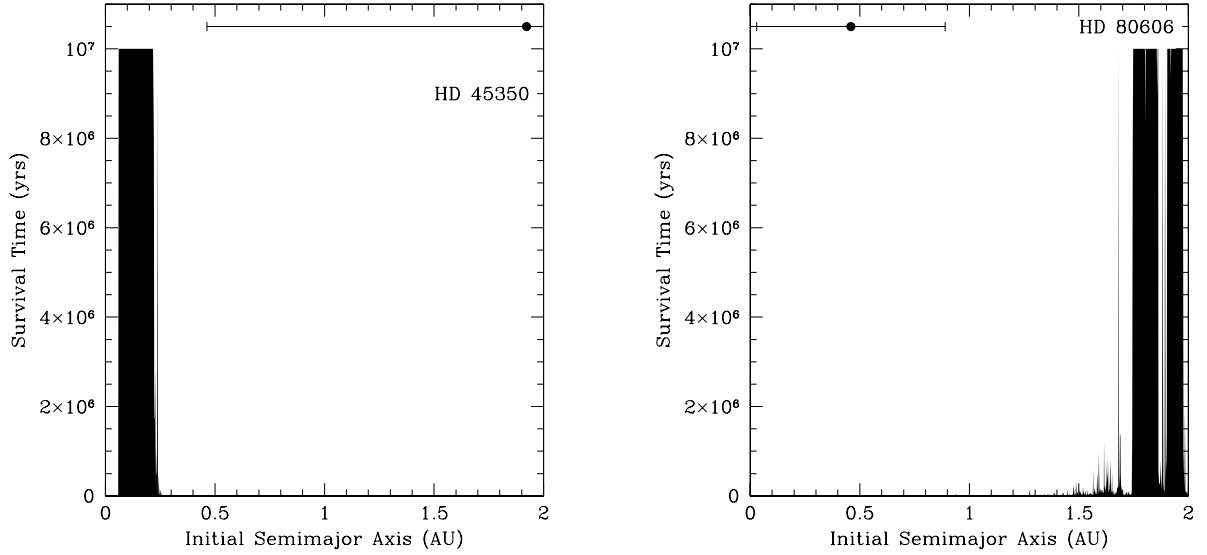


FIG. 2.— Same as Fig. 1, but for the HD 45350 (left) and HD 80606 (right) systems.

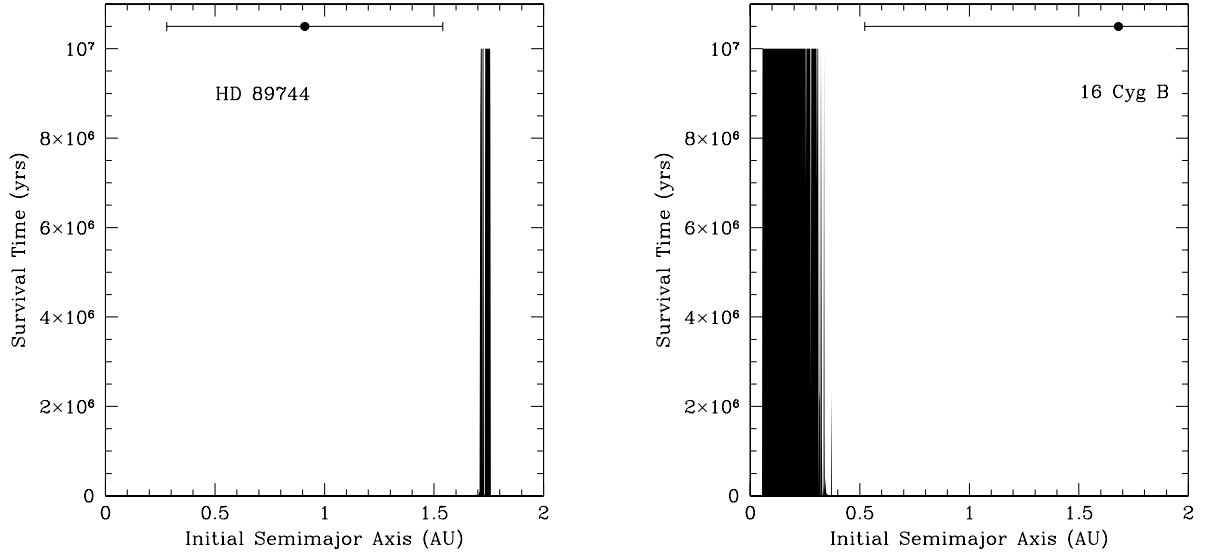


FIG. 3.— Same as Fig. 1, but for the HD 89744 (left) and 16 Cyg B (right) systems.

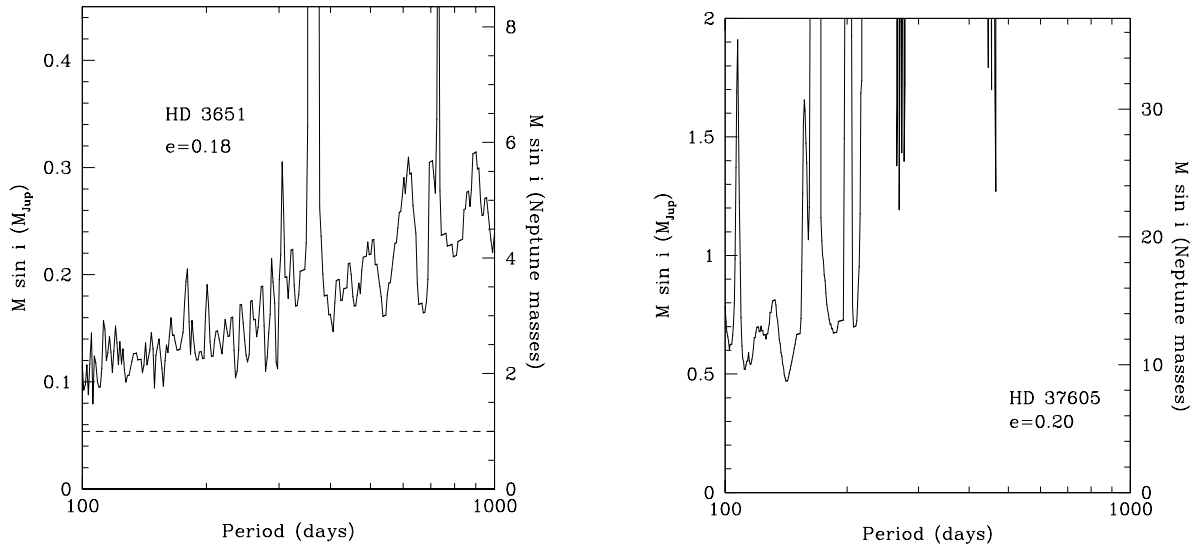


FIG. 4.— Left panel: Detection limits for additional planets in orbits with  $e = 0.18$  in the HD 3651 system. Planets in the parameter space above the plotted points are excluded at the 99% confidence level. The horizontal dashed line indicates the mass of Neptune. Right panel: Same, but for planets with  $e = 0.20$  in the HD 37605 system.



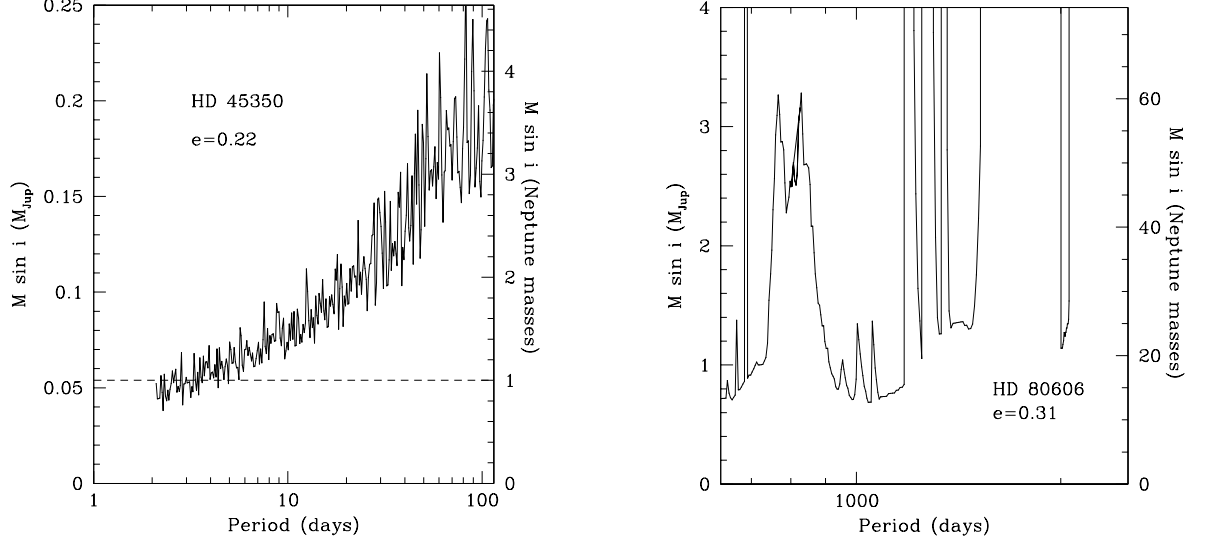


FIG. 5.— Left panel: Detection limits for additional planets with  $e = 0.22$  in the HD 45350 system. The horizontal dashed line indicates the mass of Neptune. Right panel: Same, but for planets with  $e = 0.31$  in the HD 80606 system. Planets in the parameter space above the plotted points are excluded at the 99% confidence level.

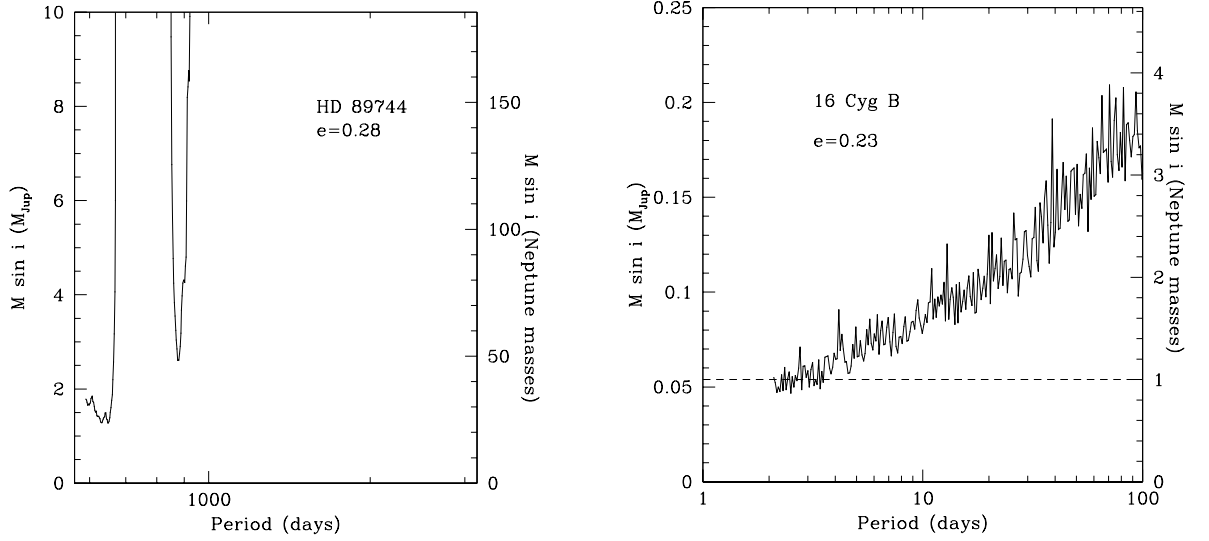


FIG. 6.— Left panel: Detection limits for additional planets with  $e = 0.28$  in the HD 89744 system. Right panel: Same, but for planets with  $e = 0.23$  in the 16 Cyg B system. The horizontal dashed line indicates the mass of Neptune. Planets in the parameter space above the plotted points are excluded at the 99% confidence level.

TABLE 3  
HET RADIAL VELOCITIES FOR HD 3651

JD-2400000	Velocity (m s <sup>-1</sup> )	Uncertainty (m s <sup>-1</sup> )
53581.87326	-19.1	2.9
53581.87586	-19.4	2.7
53581.87846	-20.7	2.7
53600.79669	-11.5	2.4
53600.79860	-15.5	3.0
53600.80050	-22.8	2.9
53604.79166	-15.8	1.9
53604.79356	-18.8	2.1
53604.79548	-21.3	2.1
53606.78169	-19.3	1.8
53606.78360	-14.8	2.1
53606.78551	-24.0	1.8
53608.77236	-18.8	1.9
53608.77426	-18.0	1.9
53608.77617	-18.8	1.8
53615.96280	-28.0	2.6
53615.96471	-31.9	2.4
53615.96662	-37.8	2.5
53628.74050	-6.8	2.2
53628.74240	-14.5	2.4
53628.74431	-5.5	2.2
53669.61012	-18.2	2.1
53669.61203	-19.2	2.2
53669.61394	-17.7	2.4
53678.78954	-10.6	2.4
53678.79141	-8.6	2.3
53678.79332	-2.3	2.1
53682.78423	-15.4	2.2
53682.78609	-15.0	2.3
53682.78801	-11.9	2.3
53687.77684	11.3	2.2
53687.77875	8.7	2.2
53687.78066	15.9	2.2
53691.75967	9.6	2.2
53691.76158	20.3	2.1
53691.76349	15.9	2.0
53696.75837	16.1	1.8
53696.76028	18.6	1.8
53696.76220	20.0	2.0
53694.75275	18.0	1.9
53694.75466	15.1	2.0
53694.75656	17.8	2.0
53955.83401	-0.5	1.9
53955.83593	-1.2	2.0
53955.83785	1.3	1.9
53956.82850	0.4	2.0
53956.83046	-1.0	2.0
53956.83236	-5.4	2.2
53957.82201	-2.1	2.0
53957.82392	-1.3	2.0
53957.82583	-3.6	2.0
53973.80721	9.8	7.3
53973.81020	3.5	2.3
53973.81200	-3.5	2.0
53976.78393	-10.4	2.4
53976.78586	-5.4	2.1
53976.78778	-6.7	2.3
53978.97197	-3.8	2.6
53985.95886	-9.0	2.3
53985.96079	4.3	3.3
53987.95335	-8.3	2.2
53987.95527	-8.0	2.2
53987.95719	-12.0	2.3
53989.73817	-13.2	2.2
53989.74009	-13.2	2.1
53989.74203	-18.6	2.1
54003.70719	2.0	2.2
54003.70915	4.7	2.4
54005.68297	7.0	2.5
54005.68488	11.1	2.0
54005.68690	10.2	2.1
54056.77919	-7.5	2.2
54056.78110	-11.5	2.1
54056.78302	-9.6	2.3
54062.55119	20.1	1.8
54062.55312	21.9	2.0
54062.55505	20.9	2.0
54064.54710	12.8	2.0
54064.54902	16.7	2.1
54064.55094	16.6	2.1

TABLE 4  
HET RADIAL VELOCITIES FOR HD 37605

JD-2400000	Velocity ( $\text{m s}^{-1}$ )	Uncertainty ( $\text{m s}^{-1}$ )
53002.67151	487.6	3.8
53003.68525	495.5	3.0
53006.66205	496.2	3.0
53008.66407	501.3	2.9
53010.80477	499.8	2.9
53013.79399	482.1	2.6
53042.72797	269.7	2.8
53061.66756	489.0	2.6
53065.64684	479.0	2.8
53071.64383	463.8	2.6
53073.63819	460.4	2.6
53082.62372	422.8	2.5
53083.59536	422.2	2.8
53088.59378	418.6	4.0
53089.59576	379.1	2.2
53092.59799	343.7	2.5
53094.58658	323.2	2.4
53095.58642	302.1	2.4
53096.58744	302.1	3.2
53098.57625	193.8	2.7
53264.95137	164.9	3.0
53265.94744	112.9	3.0
53266.94598	113.2	3.7
53266.95948	74.6	3.6
53266.97396	119.2	8.0
53283.92241	471.6	2.7
53318.81927	213.3	3.0
53335.92181	496.9	2.6
53338.90602	493.9	2.6
53377.81941	109.1	2.7
53378.81189	214.6	2.7
53379.80225	338.3	2.6
53381.64429	436.1	2.7
53384.64654	482.9	2.8
53724.85584	468.2	2.6
53731.69723	435.4	2.7
53738.67472	404.3	2.6
53743.81020	400.5	2.6
53748.64724	348.4	2.7
54039.85015	272.5	3.1
54054.96457	437.4	2.7
54055.95279	422.0	2.9
54067.76282	376.4	2.6

TABLE 5  
HET RADIAL VELOCITIES FOR HD 80606

JD-2400000	Velocity ( $\text{m s}^{-1}$ )	Uncertainty ( $\text{m s}^{-1}$ )
53346.88103	-20.8	3.0
53358.02089	-49.5	2.7
53359.82400	-60.4	3.0
53361.02985	-64.7	2.5
53365.03079	-77.4	2.4
53373.98282	-88.4	3.0
53377.80112	-105.5	2.4
53379.75230	-109.3	2.7
53389.74170	-115.3	2.5
53391.74400	-129.4	2.4
53395.72763	-146.4	2.3
53399.72518	-158.4	2.5
53401.72497	-174.7	2.7
53414.67819	-219.8	3.0
53421.85529	261.0	2.2
53423.86650	322.1	2.0
53424.85231	245.9	2.1
53432.87120	87.5	1.9
53433.60628	70.0	2.1
53446.79322	4.5	1.9
54161.85400	-109.5	2.8
54166.83797	-119.3	2.4
54186.76189	-184.2	2.3

TABLE 6  
HET RADIAL VELOCITIES FOR HD 89744

JD-2400000	Velocity (m s <sup>-1</sup> )	Uncertainty (m s <sup>-1</sup> )
53709.89685	-184.5	2.3
53723.85188	-238.6	2.2
53723.85367	-238.2	2.5
53723.85546	-227.7	2.3
53727.84394	-238.9	2.5
53727.84573	-244.9	2.4
53727.84752	-242.9	2.6
53736.81887	-257.6	2.5
53736.82100	-248.2	2.9
53736.82315	-253.4	2.4
53738.03261	-246.7	2.8
53738.03441	-243.3	2.4
53738.03620	-236.0	2.5
53738.80860	-240.5	2.6
53738.81040	-258.9	2.4
53738.81219	-249.3	2.5
53734.81795	-242.8	2.6
53734.81973	-243.9	2.8
53734.82152	-248.5	2.4
53742.79119	-252.0	2.8
53742.79299	-257.2	2.8
53742.79479	-239.7	2.8
53751.78199	-257.4	2.9
53751.78378	-263.1	2.5
53751.78558	-268.0	2.3
53753.78155	-273.1	2.5
53753.78381	-278.7	2.5
53753.78607	-266.4	2.4
53755.76038	-286.6	2.3
53755.76218	-266.5	2.6
53755.76397	-274.9	2.7
53746.81506	-257.1	1.9
53746.81778	-250.9	2.1
53746.82051	-245.2	2.3
53757.77002	-277.6	2.4
53757.77181	-280.3	2.4
53757.77360	-288.7	2.2
53797.64609	-439.8	3.1
53797.64834	-462.6	2.8
53797.65059	-452.5	2.9
53809.62428	-658.6	2.4
53809.62700	-658.8	2.5
53809.62972	-659.2	2.3
53837.76359	-304.3	3.0
53837.76670	-324.0	2.9
53837.78731	-308.6	2.7
53837.79077	-285.2	2.6
53866.69987	-215.9	1.7
53866.70329	-228.3	1.7
53866.70670	-220.4	1.8
53868.68349	-251.6	3.8
53868.68562	-208.6	2.9
53868.68777	-247.4	9.7
53875.66956	-215.7	1.6
53883.65565	-213.8	1.8
53883.65837	-209.2	1.7
53883.66109	-200.4	1.7
53890.63776	-203.4	1.7
53890.63954	-202.6	1.9
53890.64134	-203.2	1.9
53893.62959	-193.8	2.0
53893.63139	-189.3	1.9
53893.63318	-189.7	1.8
54047.94811	-375.2	4.8
54047.94991	-353.2	4.5
54047.95172	-362.6	4.4
54050.96248	-415.0	2.6
54050.96453	-423.0	2.5
54050.96657	-420.1	2.4
54052.96488	-426.8	2.3
54052.96762	-437.1	2.5
54052.97035	-447.6	2.5
54056.94606	-468.0	3.0
54056.94786	-466.4	2.6
54056.94964	-479.4	2.8
54063.92981	-599.1	2.1
54063.93166	-594.8	2.3
54063.93348	-592.3	2.4
54073.91213	-685.8	2.8
54073.91476	-688.7	2.9